

Fig. S1: Photos of the 1448 tuff in core BF before sampling. **Top:** round side of the core, **Bottom:** slabbed side of the core. The dashed rectangle marks the approximate dimensions of the sample taken. Note that the core is cut in half (slabbed) and that the other half is not available.

Table S1a: Details of sampled ashes.						
Sample name	Tuff name used in this study	Sampling location	Coordinates: WGS84 datum		Description	Depth in core BF1
			Latitude	Longitude		(ft)
GR-416	Sixth tuff	The Palisades, west of Green River, Wyoming, ~1.5 km west of Tollgate Rock.	N41°33'20"	W109°30'02"	~17 cm white layer with grey and orange staining. The ash is normally graded, and the lowermost 1.5-2 cm contains biotite crystals as coarse as 1-2 mm and hornblende crystals as coarse as 1mm. This lowermost part was processed for the U-Pb dating. Massive dark-brown mudstone (mid-grade oil shale) is below and brown mudstone (low grade oil shale) is above.	453.9
WC07-10	Layered tuff	Tollgate Rock, Green River, Wyoming	N41°32'37.4"	W109°28'59.3"	7 cm, laminated (2-3 mm thick lamina), weathered light brown or white. Biotite crystals as coarse as 0.1 mm. Oil shale bed immediately above this ash is relatively organic rich and is less organic rich below.	538.6
GR-411	Main tuff	Tollgate Rock, Green River, Wyoming	N41°32'32"	W109°28'56"	~18 cm ash within low to medium grade oil shale bed. The ash is partitioned into four layers 1, 5, 6 and 4 cm thick from bottom to top, respectively. White mud lamina 0.5-1 cm thick separates the layers. Each ash layer is composed mostly of white matrix, and is normally graded with respect to visible biotite crystals that are as coarse as 0.5 mm at the bottom of the lowermost layer. Dated sample is taken from the lowermost two layers, whereas upper layers of the same tuff did not yield any zircons.	629.6
GR-418	Grey tuff	Northwest of Rock Springs, Wyoming	N41°39'24.1"	W109°17'21.4"	See Smith et al. (2003)	972.2
GR-402	Second tuff	Firehole Canyon, Wyoming	N41°21'01.6"	W109°22'35.5"	~8 to 15 cm at sampling location, within the basal interval of an organic rich oil shale bed. Matrix is indurated white silt, weathers orange. Phenocrysts of hornblende and biotite are as coarse as 0.5 mm.	1250.3
GR-401	Firehole tuff	Firehole Canyon, Wyoming	N41°21'01.9"	W109°22'32.4"	~15 cm layer weathered orange and breaks into distinct blocky pieces. Located within the basal interval of an organic rich oil shale bed. Phenocrysts of biotite as coarse as 0.063 mm.	1389.3
GR-1448	1448 tuff	Core BF (ERDA-LERC Blacks Fork 1; USGS ID for Fischer assay data is W0080; USGS Core Research library number is E216)	41°21'23.29"N (Brownfield et al., 2011)	109°31'32.32"W (Brownfield et al., 2011)	~3 cm white layer with biotite phenocrysts at the base. Interbedded within a low grade oil shale with syneresis cracks at the base (figure S1).	1448

Table S1b: Nomenclature				
	Tuff names in these previous studies:			
Sample name	Generalized stratigraphy of the Wilkins Peak Member in Culbertson (1961)	Generalized stratigraphy of the Wilkins Peak Member in Culbertson et al. (1980)	Tuffs in core BF1 as described in Roehler (1991a)	Smith et al. (2003,2008)
GR-416	Sixth tuff	Un-named tuff at the top of oil shale bed IL13	Un-named tuff at the top of oil shale bed 77	Sixth tuff
WC07-10	Fifth tuff	Tollgate tuff	Layered tuff	Layered tuff
GR-411	Third tuff	Main tuff	Main tuff	Main tuff
GR-418	Not mentioned	Un-named tuff at the base of oil shale bed DE2	Un-named tuff at the base of oil shale bed 38	Grey tuff
GR-402	Second tuff	Un-named tuff at the base of oil shale bed A1	Un-named tuff at the base of oil shale bed 20	Not mentioned
GR-401	First tuff	Firehole tuff	Firehole tuff	Firehole tuff
GR-1448	Not mentioned	Un-named tuff at the top of oil shale bed TF4	Although this core was described, this ash was not indicated in the publication	Not mentioned

TABLE S2

U-Pb data for analyzed zircon from tuff samples of Green River Formation, Wyoming.

Sample	Composition					Ratios						Age (Ma)				corr.
	Pb _c [‡]	Pb ^{+‡}	Th	²⁰⁶ Pb [§]	²⁰⁸ Pb [#]	²⁰⁶ Pb ^{††}	err	²⁰⁷ Pb ^{††}	err	²⁰⁷ Pb ^{††}	err	²⁰⁶ Pb	err	²⁰⁷ Pb	²⁰⁷ Pb	
Fractions [†]	(pg)	Pb _c	U	²⁰⁴ Pb	²⁰⁶ Pb	²³⁸ U	(2σ%)	²³⁵ U	(2σ%)	²⁰⁶ Pb	(2σ%)	²³⁸ U	(2σ)	²³⁵ U	²⁰⁶ Pb	coef.
GR-416 – Sixth tuff																
z3	0.4	8.8	0.50	545.1	0.161	0.007730	(.18)	0.04976	(2.10)	0.04671	(2.08)	49.642	0.089	49.3	33	0.17
z2	0.5	10.4	0.54	635.6	0.174	0.007731	(.16)	0.05049	(1.74)	0.04739	(1.73)	49.645	0.081	50.01	68	0.15
z1	0.7	4.8	0.54	302.1	0.174	0.007740	(.26)	0.05015	(3.59)	0.04702	(3.53)	49.70	0.13	49.7	49	0.26
z6	0.5	9.3	0.53	571.8	0.169	0.007740	(.16)	0.05027	(1.86)	0.04712	(1.82)	49.702	0.078	49.80	54	0.30
z4	0.4	9.9	0.52	611.5	0.166	0.007740	(.14)	0.05050	(1.72)	0.04734	(1.68)	49.705	0.068	50.02	65	0.27
z7	0.6	7.3	0.54	451.6	0.172	0.007742	(.18)	0.05064	(2.29)	0.04746	(2.25)	49.714	0.087	50.2	71	0.26
WC07-10 – Layered tuff																
z7	0.2	2.7	0.31	189.8	0.100	0.007746	(.64)	0.05105	(11.2)	0.04782	(10.8)	49.74	0.32	50.6	89	0.62
z9	0.3	4.5	0.29	302.5	0.094	0.007755	(.31)	0.04929	(4.18)	0.04612	(4.06)	49.80	0.15	48.9	3	0.41
z6	0.4	2.3	0.44	161.1	0.141	0.007773	(.52)	0.04962	(7.53)	0.04632	(7.40)	49.91	0.26	49.2	13	0.27
z2	0.3	6.2	0.35	405.8	0.111	0.007772	(.20)	0.05066	(2.55)	0.04729	(2.51)	49.91	0.10	50.2	63	0.25
z3	0.7	7.0	0.30	459.1	0.098	0.007774	(.17)	0.05102	(2.21)	0.04762	(2.17)	49.919	0.086	50.5	80	0.26
z1	0.5	9.7	0.33	629.7	0.105	0.007775	(.15)	0.05098	(1.69)	0.04757	(1.65)	49.926	0.072	50.48	77	0.30
z4	0.7	6.6	0.32	436.0	0.103	0.007782	(.18)	0.05082	(2.36)	0.04739	(2.32)	49.972	0.092	50.3	68	0.25
z8	0.3	1.4	0.27	109.7	0.088	0.007783	(.94)	0.04905	(13.5)	0.04573	(13.1)	49.98	0.47	48.6	0	0.43
GR-411 – Main tuff																
z9	0.5	3.9	0.61	247.0	0.195	0.007773	(.36)	0.05037	(4.90)	0.04701	(4.78)	49.92	0.18	49.9	49	0.39
z5	0.2	7.9	1.16	424.4	0.370	0.007786	(.32)	0.05059	(4.92)	0.04714	(4.71)	50.00	0.16	50.1	55	0.68
z3	0.4	14.6	1.18	760.2	0.377	0.007798	(.13)	0.05035	(1.44)	0.04686	(1.41)	50.072	0.065	49.88	41	0.30
z2	0.3	17.3	0.59	1032.7	0.188	0.007804	(.10)	0.05099	(1.04)	0.04742	(1.01)	50.110	0.050	50.50	69	0.32
z1	0.3	9.6	0.98	527.5	0.313	0.007804	(.17)	0.05037	(2.15)	0.04684	(2.10)	50.112	0.087	49.9	40	0.31

Sample	Composition					Ratios						Age (Ma)				corr.
	Pb _c [‡]	Pb ^{*‡}	Th	²⁰⁶ Pb [§]	²⁰⁸ Pb [#]	²⁰⁶ Pb ^{††}	err	²⁰⁷ Pb ^{††}	err	²⁰⁷ Pb ^{††}	err	²⁰⁶ Pb	err	²⁰⁷ Pb	²⁰⁷ Pb	
Fractions [†]	(pg)	Pb _c	U	²⁰⁴ Pb	²⁰⁶ Pb	²³⁸ U	(2σ%)	²³⁵ U	(2σ%)	²⁰⁶ Pb	(2σ%)	²³⁸ U	(2σ)	²³⁵ U	²⁰⁶ Pb	coef.
z7	0.2	17.1	0.50	1044.1	0.160	0.007806	(.10)	0.05025	(1.28)	0.04672	(1.25)	50.123	0.051	49.79	34	0.33
z4	0.3	11.6	1.32	589.6	0.422	0.007808	(.16)	0.05092	(1.79)	0.04732	(1.75)	50.136	0.079	50.43	64	0.32
z10	0.5	5.2	1.17	285.4	0.374	0.007808	(.29)	0.05038	(3.93)	0.04682	(3.85)	50.14	0.15	49.9	39	0.31
GR-418 – Grey tuff																
z4	0.4	47.7	0.55	2851.5	0.175	0.007907	(.07)	0.05145	(.44)	0.04722	(.41)	50.769	0.035	50.94	59.2	0.40
z8	0.4	52.9	0.64	3081.1	0.205	0.007915	(.06)	0.05139	(.42)	0.04711	(.41)	50.825	0.031	50.89	53.8	0.30
z6	0.3	20.4	0.46	1259.0	0.149	0.007916	(.09)	0.05161	(.88)	0.04731	(.85)	50.827	0.046	51.09	64	0.39
z7	0.2	18.2	1.21	937.8	0.387	0.007917	(.14)	0.05147	(1.19)	0.04717	(1.15)	50.837	0.070	50.96	57	0.36
z9	0.2	54.5	0.81	3047.3	0.258	0.007918	(.07)	0.05136	(.40)	0.04706	(.38)	50.845	0.033	50.86	51.4	0.40
z1	0.7	25.1	0.48	1533.0	0.153	0.007919	(.07)	0.05140	(.73)	0.04710	(.72)	50.846	0.037	50.90	53	0.22
z14	0.2	15.4	0.70	897.2	0.223	0.007919	(.15)	0.05103	(1.83)	0.04675	(1.74)	50.850	0.077	50.53	35	0.61
z10	0.2	26.9	0.48	1644.6	0.154	0.007919	(.07)	0.05139	(.74)	0.04708	(.73)	50.850	0.035	50.88	52	0.21
z12	0.2	51.8	0.33	3279.1	0.105	0.007923	(.06)	0.05130	(.39)	0.04698	(.36)	50.876	0.032	50.80	47.2	0.40
z15	0.6	9.3	0.58	565.0	0.187	0.007924	(.14)	0.05188	(1.80)	0.04751	(1.76)	50.883	0.072	51.36	74	0.27
z2	0.4	81.7	0.35	5136.3	0.111	0.007924	(.06)	0.05149	(.25)	0.04715	(.23)	50.883	0.031	50.98	55.7	0.45
z17	0.5	10.3	0.88	578.2	0.282	0.007929	(.14)	0.05216	(1.83)	0.04773	(1.80)	50.910	0.073	51.63	85	0.26
z16	0.6	8.9	0.61	540.9	0.194	0.007929	(.16)	0.05196	(1.95)	0.04755	(1.91)	50.911	0.081	51.44	76	0.33
z11	0.2	34.0	0.60	2007.4	0.193	0.007935	(.08)	0.05172	(.78)	0.04729	(.76)	50.950	0.042	51.20	63	0.36
z5	0.5	35.0	0.38	2189.3	0.123	0.007936	(.07)	0.05157	(.54)	0.04715	(.51)	50.960	0.038	51.06	56	0.42
z3	0.5	47.0	0.39	2895.1	0.125	0.011535	(.08)	0.09571	(.37)	0.06021	(.34)	73.93	0.06	92.81	610.1	0.43
GR-402 – Second tuff																
z7	0.4	13.0	0.31	841.4	0.100	0.007980	(.11)	0.05165	(1.31)	0.04697	(1.28)	51.239	0.056	51.14	46	0.31
z8	0.4	10.1	0.36	650.0	0.115	0.007981	(.13)	0.05188	(1.63)	0.04716	(1.60)	51.248	0.068	51.35	56	0.27
z4	0.8	5.5	0.28	366.6	0.090	0.007981	(.27)	0.05250	(3.24)	0.04773	(3.19)	51.25	0.14	52.0	85	0.22

Sample	Composition					Ratios						Age (Ma)				corr.
	Pb _c [‡]	Pb ^{*‡}	Th	²⁰⁶ Pb [§]	²⁰⁸ Pb [#]	²⁰⁶ Pb ^{††}	err	²⁰⁷ Pb ^{††}	err	²⁰⁷ Pb ^{††}	err	²⁰⁶ Pb	err	²⁰⁷ Pb	²⁰⁷ Pb	
Fractions [†]	(pg)	Pb _c	U	²⁰⁴ Pb	²⁰⁶ Pb	²³⁸ U	(2σ%)	²³⁵ U	(2σ%)	²⁰⁶ Pb	(2σ%)	²³⁸ U	(2σ)	²³⁵ U	²⁰⁶ Pb	coef.
z5	0.4	22.6	0.29	1460.4	0.092	0.007983	(.10)	0.05191	(.82)	0.04718	(.77)	51.259	0.049	51.39	57	0.51
z6	0.5	16.2	0.36	1031.4	0.114	0.007987	(.09)	0.05216	(.98)	0.04739	(.96)	51.281	0.048	51.62	68	0.24
z9	0.3	12.5	0.31	809.3	0.099	0.007989	(.12)	0.05189	(1.33)	0.04713	(1.29)	51.296	0.063	51.37	55	0.36
z11	0.4	20.0	0.38	1262.6	0.121	0.007991	(.08)	0.05208	(.81)	0.04729	(.80)	51.308	0.041	51.55	63	0.19
z3	0.5	4.2	0.26	286.7	0.082	0.007992	(.32)	0.05175	(3.98)	0.04698	(3.87)	51.32	0.16	51.2	47	0.37
z10	0.6	4.3	0.28	294.1	0.088	0.008003	(.27)	0.05179	(3.63)	0.04696	(3.56)	51.39	0.14	51.3	46	0.27
z1	0.3	6.2	0.26	417.2	0.084	0.008022	(.23)	0.05247	(2.62)	0.04746	(2.55)	51.51	0.12	51.9	72	0.32
z2	0.8	48.9	0.25	3170.6	0.079	0.009912	(.10)	0.06507	(.37)	0.04763	(.35)	63.585	0.064	64.01	79.9	0.33
GR-401 – Firehole tuff																
z1	0.4	33.5	0.42	2078.7	0.134	0.008017	(.07)	0.05190	(.57)	0.04698	(.56)	51.475	0.036	51.38	47	0.20
z15	0.3	12.8	0.42	807.3	0.134	0.008018	(.11)	0.05193	(1.36)	0.04700	(1.33)	51.479	0.059	51.40	48	0.29
z9	0.2	47.7	0.35	3010.9	0.111	0.008024	(.06)	0.05197	(.42)	0.04700	(.41)	51.518	0.032	51.44	47.9	0.24
z7	0.3	22.6	0.41	1412.5	0.132	0.008024	(.09)	0.05214	(.87)	0.04715	(.83)	51.520	0.049	51.61	56	0.44
z8	0.2	31.6	0.41	1966.7	0.131	0.008024	(.08)	0.05188	(.68)	0.04692	(.66)	51.521	0.041	51.36	44	0.33
z14	0.2	77.7	0.47	4723.2	0.151	0.008024	(.05)	0.05197	(.27)	0.04700	(.25)	51.522	0.027	51.45	47.9	0.42
z13	0.3	17.1	0.35	1088.6	0.112	0.008025	(.10)	0.05222	(1.07)	0.04721	(1.04)	51.527	0.051	51.68	59	0.40
z16	0.2	17.7	0.32	1137.7	0.103	0.008025	(.10)	0.05222	(1.08)	0.04722	(1.04)	51.528	0.049	51.69	59	0.41
z12	0.3	16.1	0.40	1013.3	0.128	0.008026	(.11)	0.05192	(1.19)	0.04694	(1.15)	51.531	0.055	51.39	45	0.41
z4	0.4	18.1	0.37	1144.2	0.118	0.008027	(.09)	0.05180	(.97)	0.04683	(.95)	51.538	0.047	51.28	39	0.23
z3	0.3	34.7	0.37	2177.9	0.118	0.008030	(.09)	0.05197	(.56)	0.04696	(.55)	51.557	0.044	51.44	46	0.22
z6	0.3	31.2	0.39	1948.2	0.124	0.008030	(.08)	0.05205	(.69)	0.04703	(.66)	51.557	0.039	51.52	50	0.43
z11	0.4	27.3	0.38	1711.4	0.123	0.008033	(.08)	0.05221	(.65)	0.04716	(.63)	51.576	0.039	51.68	56	0.37
z10	0.6	10.0	0.42	631.7	0.133	0.008040	(.13)	0.05217	(1.67)	0.04708	(1.63)	51.622	0.069	51.64	52	0.31

Sample	Composition					Ratios						Age (Ma)				corr.
	Pb _c [‡]	Pb ^{*‡}	Th	²⁰⁶ Pb [§]	²⁰⁸ Pb [#]	²⁰⁶ Pb ^{††}	err	²⁰⁷ Pb ^{††}	err	²⁰⁷ Pb ^{††}	err	²⁰⁶ Pb	err	²⁰⁷ Pb	²⁰⁷ Pb	
Fractions [†]	(pg)	Pb _c	U	²⁰⁴ Pb	²⁰⁶ Pb	²³⁸ U	(2σ%)	²³⁵ U	(2σ%)	²⁰⁶ Pb	(2σ%)	²³⁸ U	(2σ)	²³⁵ U	²⁰⁶ Pb	coef.
GR-1448m – 1448 tuff																
z2	1.3	0.9	0.47	75.1	0.149	0.007981	(1.25)	0.05149	(17.4)	0.04681	(17.2)	51.25	0.64	51.0	39	0.25
z3	0.5	1.5	0.40	110.7	0.128	0.007994	(.80)	0.05045	(11.6)	0.04580	(11.4)	51.33	0.41	50.0	0	0.28
z9	0.8	1.4	0.30	109.5	0.097	0.008001	(.87)	0.05073	(12.5)	0.04600	(12.2)	51.37	0.44	50.2	0	0.40
z1	0.6	7.7	0.66	461.2	0.210	0.008031	(.18)	0.05165	(2.32)	0.04667	(2.26)	51.564	0.094	51.1	31	0.32
z4	0.5	11.4	0.43	714.6	0.137	0.008036	(.13)	0.05225	(1.53)	0.04718	(1.48)	51.594	0.066	51.72	57	0.38
z10	0.4	1.3	0.35	103.0	0.111	0.008052	(.88)	0.05171	(12.0)	0.04659	(11.8)	51.70	0.45	51.2	27	0.28
z8	0.4	1.6	0.63	113.6	0.201	0.008078	(.78)	0.05694	(10.2)	0.05115	(10.0)	51.87	0.40	56.2	246	0.31
z5	1.1	123.2	0.37	7354.3	0.110	0.236770	(.06)	3.55785	(.12)	0.10903	(.08)	1369.9	0.70	1540.18	1782.5	0.73
z12	0.7	70.6	0.19	4419.3	0.054	0.286089	(.10)	4.31608	(.20)	0.10947	(.15)	1622.0	1.4	1696.4	1789.7	0.70
z11	0.7	76.9	0.44	4522.9	0.130	0.296291	(.08)	4.42206	(.19)	0.10829	(.15)	1672.9	1.1	1716.5	1770.1	0.65
z6	0.6	109.8	0.58	6256.6	0.168	0.303012	(.09)	4.54443	(.18)	0.10882	(.13)	1706.2	1.4	1739.1	1779.0	0.67

Notes: Corr. coef. = correlation coefficient. Age calculations are based on the decay constants of Jaffey et al. (1971).

[†] All analyses are single zircon grains and pre-treated by the thermal annealing and acid leaching (CA-TIMS) technique. Data used in age calculations are in bold.

[‡] Pb_c is total common Pb in analysis. Pb* is radiogenic Pb concentration.

[§] Measured ratio corrected for spike and fractionation only.

[#] Radiogenic Pb ratio.

^{††} Corrected for fractionation, spike, blank, and initial Th/U disequilibrium in magma. Mass fractionation correction of 0.25%/amu ± 0.04%/amu (atomic mass unit) was applied to single-collector Daly analyses. All common Pb is assumed to be blank. Total procedural blank was less than 0.1pg for U. Blank isotopic composition: ²⁰⁶Pb/²⁰⁴Pb = 18.42 ± 0.35, ²⁰⁷Pb/²⁰⁴Pb = 15.36 ± 0.23, ²⁰⁸Pb/²⁰⁴Pb = 37.46 ± 0.74.

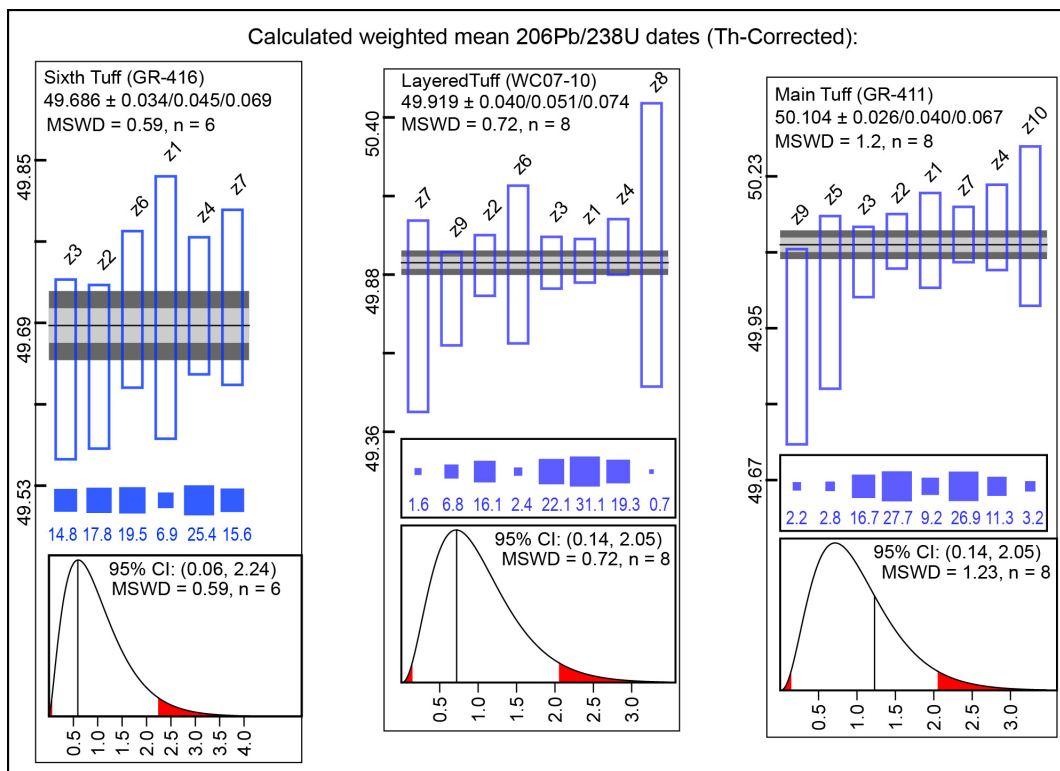


Fig. S2: Zircon date distribution plots showing calculated weighted mean dates. Bar heights are proportional to 2σ analytical uncertainty of individual zircon analyses. Horizontal bands signify weighted mean date and its uncertainty at 1σ (light shading) and 2σ (dark shading) levels. Middle box displays percentage of contribution to the mean of each analysis. Lower box shows the distribution of mean square of weighted deviates (MSWD) within 95% confidence interval. The uppermost three ashes are shown on this page, and the lower four ashes are shown in the next page.

Continued on next page....

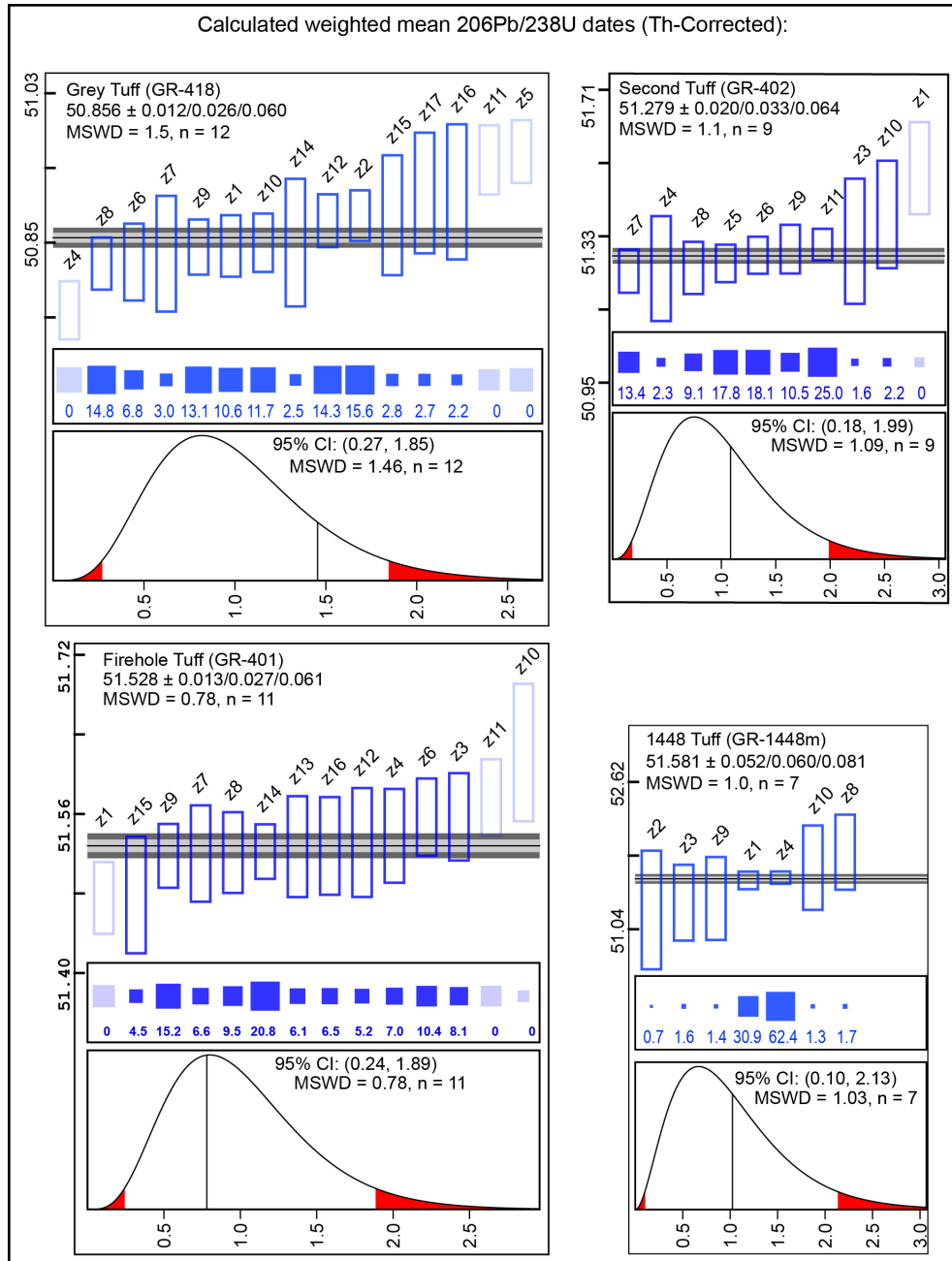
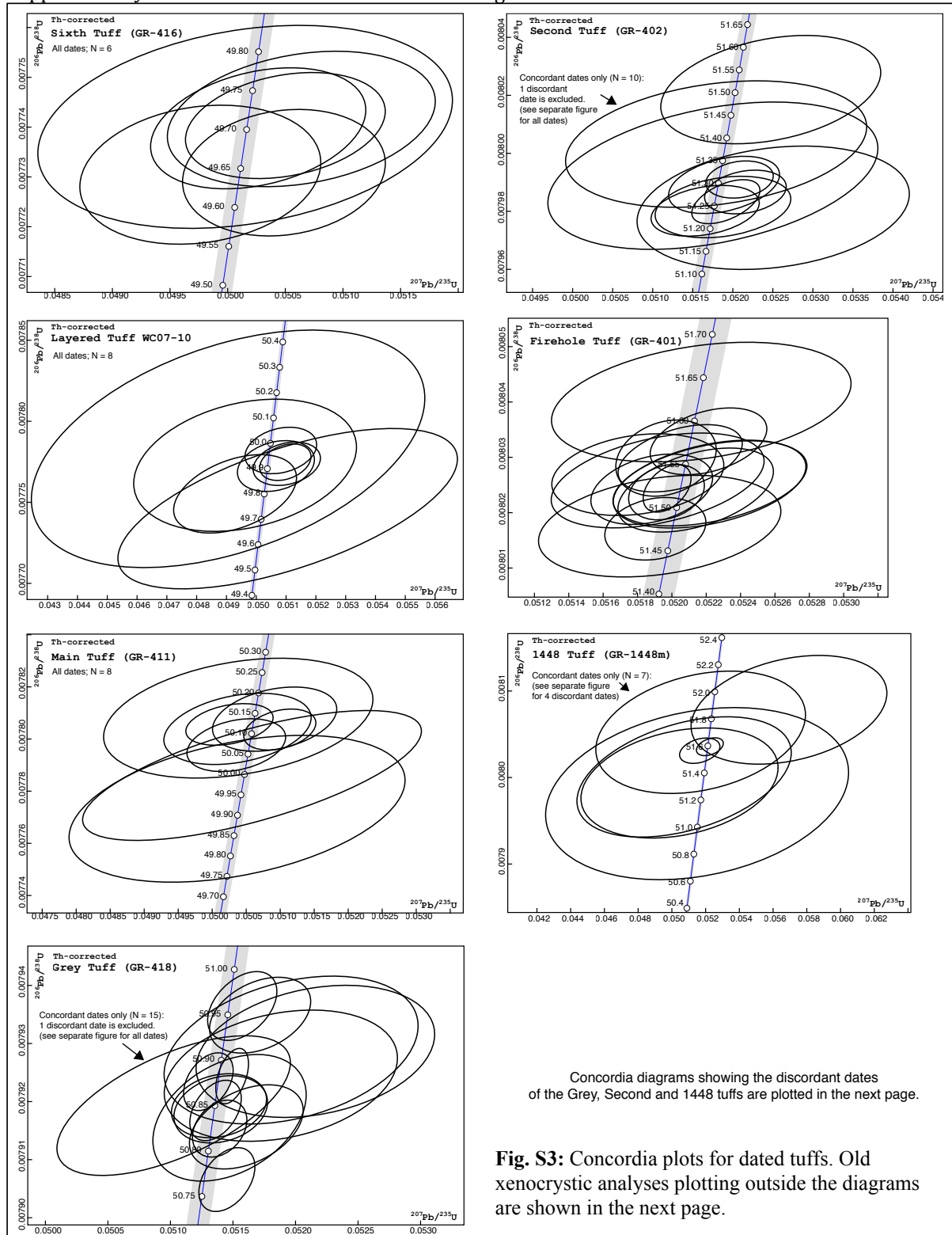


Fig. S2: Continued from previous page.



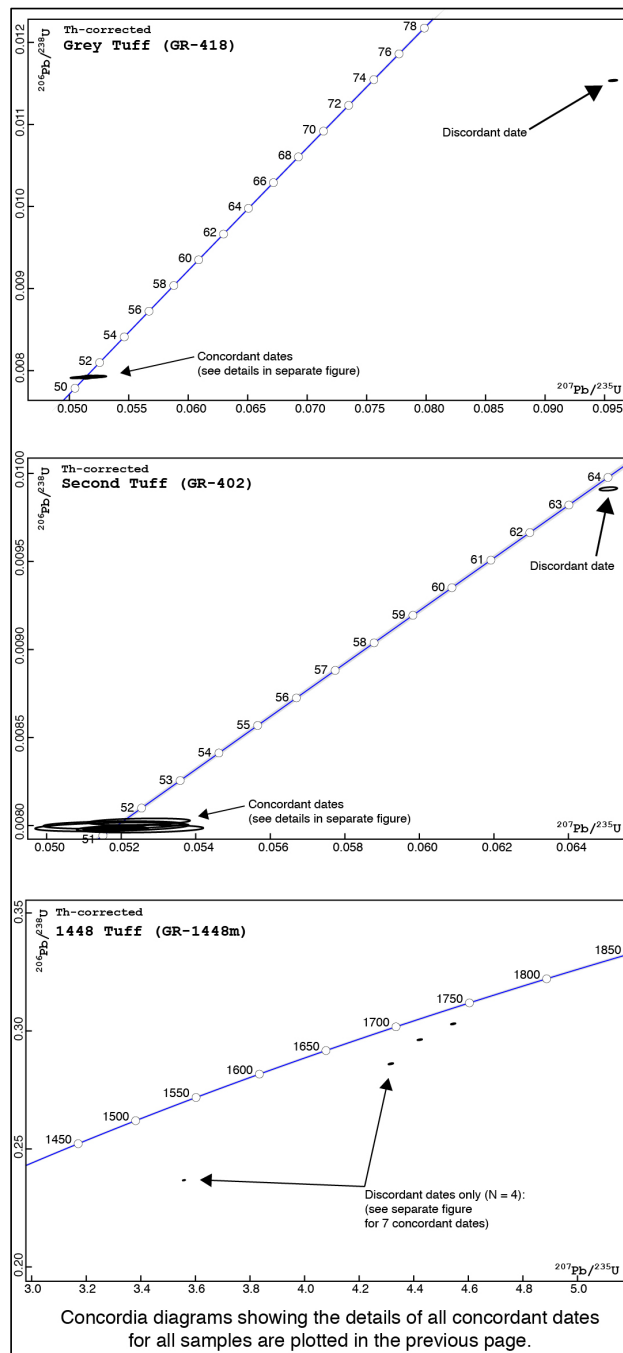


Fig. S3 (Continued from previous page): Extended Concordia plots showing old xenocrystic analyses (marked with arrows) excluded from date calculation.

Section S5.2: Details of estimating the eruption age: supplementary information for section 5.2 of the main text

We outline the general approach for the selection of analyses to include in the weighted mean in sections 5.2 of the main text and add sections with the details for each ash sample.

Details of weighted mean calculations

For full transparency in the age interpretation process, details of how the selection of crystals for the weighted mean calculations were made are given for each of the ashes in the following. All weighted mean dates are models that assume there is a single population with normally distributed errors. A common practice is to first eliminate obvious outliers and then examine the distribution of dates that remain. Dates that are distinctly younger are generally interpreted to reflect residual Pb-loss not removed by chemical abrasion and ones that are older to reflect either incorporation of whole older grains, perhaps from slightly older rocks in the source area or a mixture of core and rim. One can then investigate the sensitivity of the analyses not included in the weighted mean by adding them in. If the MSWD is within the 95% confidence interval of its distribution (with value depending on the number of analyses and approaching 1 for a large number), it indicates that the scatter or dispersion in the data can be explained by analytical uncertainties alone; however it could mask real variability that would only be obvious if the analytical uncertainties were much lower. See figure S3 for the contribution of each individual date to the weighted mean date and for the distribution of the MSWD.

The uppermost three ashes

For each of the three uppermost ashes, the dates of all zircon analyses overlap (Fig. 4a, b, c) and therefore all analyses are included in the weighted mean. Our interpreted eruption/depositional ages for these ashes are: 49.686 ± 0.034 Ma for the Sixth tuff, ($n = 6$); 49.919 ± 0.040 Ma for the Layered tuff, ($n = 8$); and 50.104 ± 0.026 Ma for the Main tuff, ($n = 8$). See Table 1 for external uncertainties.

The Grey tuff

Of the 16 crystals analyzed there are four analyses interpreted as outliers (Fig. 4d, Table S2). The most obvious is a discordant grain (z3, $^{207}\text{Pb}/^{206}\text{U}$ age of 610 Ma, Table S2) that may reflect a core within a magmatic grain. Three other grains are not included in the weighted mean plot, z4, z5, and z11. The latter two are distinctly older than the remaining 12 and the former distinctly younger. If we explore what happens when we add in the three analyses not included the weighted mean date, the calculated mean shifts from $50.856 \pm 0.012/0.026/0.060$ with MSWD of 1.5 to $50.862 \pm 0.011/0.025/0.060$ with MSWD of 6.4. The bottom line is that the calculated date and uncertainty are essentially the same but the three analyses add considerable scatter.

It is possible, though unlikely, that the youngest grain of the Grey tuff is part of a younger age population that is not represented by the remaining analyses. Some authors rely on the date of the youngest crystal(s) as the best estimate for the eruption age (e.g., Sageman et al., 2014, Wotzlaw et al., 2014), however those studies report a much wider range of dates compared the cluster of dates in this study. The ultimate test of our approach and any other geochronological

method that utilizes weighted mean dates is whether the dates of closely spaced ashes violate stratigraphic superposition. We consider the weighted mean date of 50.856 ± 0.012 Ma ($n = 12$) to represent the eruption age.

The Second tuff

The weighted mean calculation for this sample (Fig. 4e, Table S2) follows the same arguments as for the Grey tuff. An obviously older grain is rejected first (z2, $^{206}\text{Pb}/^{238}\text{U}$ age of ~ 64 Ma, Table S2) and the second oldest date is not included as well (oldest date in Fig. 4e, colored grey). If the latter is included the weighted mean date is $51.286 \pm 0.02/0.033/0.064$ with an MSWD of 2.5. If it is eliminated, the weighted mean is $51.279 \pm 0.02/0.033/0.064$ and an MSWD of 1.1. Our interpreted eruption/depositional age for this ash is 51.279 ± 0.020 Ma ($n = 9$).

The Firehole tuff

A cluster of 14 dates for the Firehole tuff highlights some of the issues involved in calculating a weighted mean date. All fourteen analyses yield a weighted mean date of $51.529 \pm 0.011/0.027/0.061$ with a MSWD of 2.3. If the oldest grain (z10) is not included the weighted mean date becomes $51.527 \pm 0.11/0.027/0.061$ Ma and a MSWD of 1.9. If the two oldest grains are removed the date shifts to $51.522 \pm (0.012/0.027/0.061)$ and a MSWD of 1.4 and finally if the two oldest and one youngest are not included, the weighted mean date is $51.528 \pm 0.013/0.027/0.061$ with a MSWD of 0.78. We choose to use $51.528 \pm 0.013/0.027/0.061$ $N = 11$, MSWD = 0.78 as the best estimate of the eruption/depositional age. If one were to make the assumption that the youngest grain is the true age, it would be 51.475 ± 0.036 Ma, but our interpretation is that this date reflects Pb-loss and should be excluded.

The 1448 tuff

Because this sample was from a drill core and is very small (<10 g) it was necessary to analyze all recovered grains. Accordingly four zircons clearly reflect inheritance of older zircon ($^{206}\text{Pb}/^{238}\text{U}$ ages > 1.3 Ga, Table S2). The remaining seven grains yield a weighted mean date of 51.581 ± 0.052 Ma (Fig. 4g, Table 1) and is our best estimate for the eruption age.

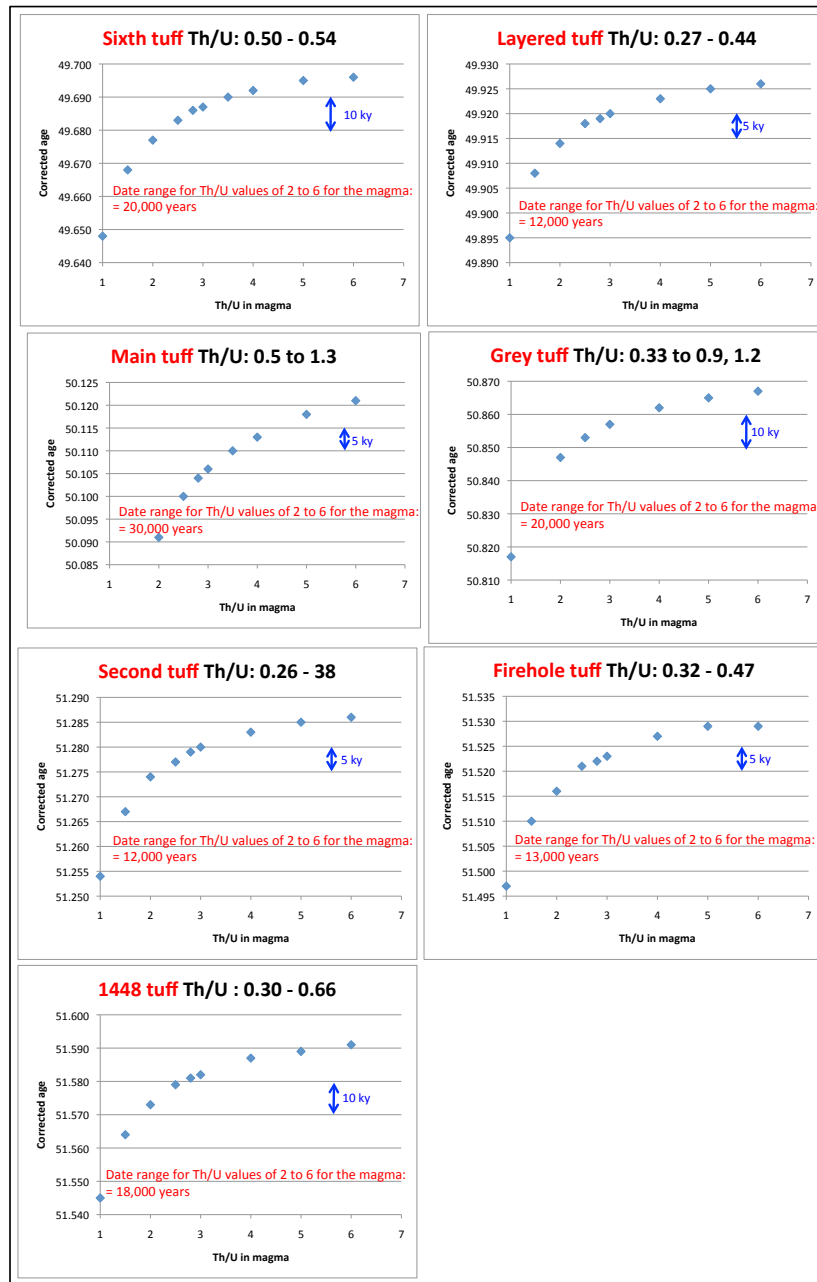


Fig. S4: The effect of variable Th/U values in the parent magma on the calculated dates. The dates shown are the calculated weighted mean dates, but the Th-correction is applied to all individual zircon dates.

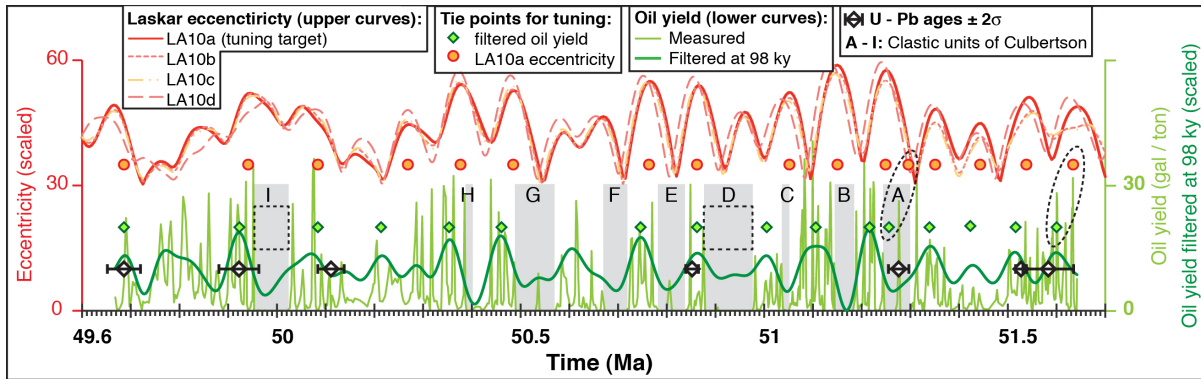


Fig. S5: Details of tuning the filtered oil yield record to the eccentricity curve LA2010a. The tuned record is constructed by aligning the diamonds marked above the filtered oil yield curve (bottom thick line) with the circles marked below the eccentricity curve, using AnalySeries (Paillard et al., 1996; e.g., see dashed ellipses connecting tie points before alignment). Lower thin curve is the original oil yield curve whereas the lower darker curve is the scaled filtered oil yield record that is filtered at frequency of 10.2 ± 5 cycles/my (i.e. center period of ~ 98 ky between periods of ~ 66 ky and ~ 192 ky). Eccentricity curves LA2010a-d are from Laskar et al. (2011a), and include the nominal solution (from file LA10a_ecc3; LA10a; solid line) and other solutions LA10b (short dashed), LA10c (dot-dashed) and LA10d (long dashed). The clastic units A through I (Culbertson, 1961) are denoted by grey vertical bars over the oil yield curves. Lowermost black diamonds mark U-Pb ages with 2σ uncertainties. Dashed rectangles below marker units D and I show intervals with no oil yield data that correspond to approximately two eccentricity cycles (after the tuning is performed). Additional intervals of no or little oil yield data correspond with the other clastic units of Culbertson (1961). Note that this tuning is only meant as an ad-hoc model to optimize selection of the next sampled ash, and it is not intended as an interpretation connecting eccentricity to lake level fluctuation as Smith et al. (2010) suggested. We acknowledge that this is an interesting suggestion that deserves further scrutiny in the future. The Smith et al. (2010) hypothesis cannot be falsified or verified by the new reported ages, because more ages would be required for a rigorous test of this hypothesis. Also, the Smith et al. (2010) hypothesis was based on Ar geochronology that although overlapping with the reported ages within external uncertainties, yields much different age/depth curve when only analytical uncertainties are taken into account. Smith also relied on a previous Laskar solution for eccentricity that is different from the most updated solution shown above. For these reasons we re-emphasize that we are not testing the Smith et al. (2010) hypothesis. Future work should allow it to be re-tested with updated eccentricity calculations as well as with more precise ages and additional dated ashes. In the meantime there is enough freedom for several options for tuning. In this study, without assuming a geological interpretation, we matched curve maxima as a simple option.

References cited in supplementary data:

- Bowring, J.F., McLean, N.M., Bowring, S.A., 2011. Engineering cyber infrastructure for U-Pb geochronology: Tripoli and U-Pb_Redux. *Geochemistry, Geophysics, Geosystems* 12, Q0AA19.
- Brownfield, M.E., Self, J.G., Mercier, T.J., 2011. Fischer assay histograms of oil-shale drill cores and rotary cuttings from the Great Divide, Green River, and Washakie Basins, Southwestern Wyoming. In U.S. Geological Survey Oil Shale Assessment Team (Eds.), *Oil shale resources of the Eocene Green River Formation, Greater Green River Basin, Wyoming, Colorado, and Utah*. U.S. Geological Survey Digital Data Series DDS-69-DD, chapter 6, 6 p.
- Culbertson, W.C., 1961. Stratigraphy of the Wilkins Peak member of the Green River Formation, Firehole Basin Quadrangle, Wyoming, Article 348. U. S. Geological Survey Professional Paper 424-D, 170-173.
- Culbertson, W.C., Smith, J.W., Trudell, L.G., 1980. Oil Shale Resources and Geology of the Green River Formation in the Green River Basin, Wyoming. Laramie Energy Technology Center LETC/RI-80/6. 102 pp.
- Jaffey, A.H., Flynn, K.F., Glendenin, L.E., Bentley, W.C., Essling, A.M., 1971. Precision Measurement of Half-Lives and Specific Activities of ^{235}U and ^{238}U . *Physical Review C* 4, 1889-1906.
- Laskar, J., Fienga, A., Gastineau, M., Manche, H., 2011a. La2010: A new orbital solution for the long-term motion of the Earth. *Astronomy and Astrophysics* 532, A89.
- McLean, N.M., Bowring, J.F., Bowring, S.A., 2011. An algorithm for U-Pb isotope dilution data reduction and uncertainty propagation, *Geochemistry, Geophysics, Geosystems* 12, Q0AA18.
- Paillard, D., Labeyrie, L., Yiou, P., 1996. Macintosh program performs time-series analysis. *EOS Transactions AGU* 77, 379.
- Roehler, H.W., 1991a. Identification of oil shale and trona beds and their geophysical log responses in the Energy Research and Development Administration Blacks Fork No. 1 corehole, Eocene Green River Formation, southwest Wyoming. U. S. Geological Survey Miscellaneous Field Studies Map MF-2158, 1 sheet.
- Sageman, B.B., Singer, B.S., Meyers, S.R., Siewert, S.E., Walaszczyk, I., Condon, D.J., Jicha, B.R., Obradovich, J.D., Sawyer, D.A., 2014. Integrating $^{40}\text{Ar}/^{39}\text{Ar}$, U-Pb, and astronomical clocks in the Cretaceous Niobrara Formation, Western Interior Basin, USA. *Geological Society of America Bulletin* 126, 956-973.
- Smith, M.E., Singer, B., Carroll, A.R., 2003. $^{40}\text{Ar}/^{39}\text{Ar}$ geochronology of the Eocene Green River Formation, Wyoming: *Geological Society of America Bulletin* 115, 549-565.
- Smith, M.E., Carroll, A.R., Singer, B.S., 2008. Synoptic reconstruction of a major ancient lake system; Eocene Green River Formation, western United States. *Geological Society of America Bulletin* 120, 54-84.
- Smith, M.E., Chamberlain, K.R., Singer, B.S., Carroll, A.R., 2010. Eocene clocks agree; coeval $^{40}\text{Ar}/^{39}\text{Ar}$, U-Pb, and astronomical ages from the Green River Formation. *Geology* 38, 527-530.
- Wotzlaw, J.F., Guex, J., Bartolini, A., Gallet, Y., Krystyn, L., McRoberts, C.A., Taylor, D., Schoene, B., Schaltegger, U., 2014. Towards accurate numerical calibration of the Late Triassic: High-precision U-Pb geochronology constraints on the duration of the Rhaetian. *Geology* 42, 571-574.